Oncogene (2020) 39:1696–1709
https://doi.org/10.1038/s41388-019-1092-z

ARTICLE

Hsa_circ_0001361 promotes bladder cancer invasion and metastasis through miR-491-5p/MMP9 axis

Feng Liu[1] · Hui Zhang[1] · Fei Xie[1,2] · Dan Tao[3] · Xingyuan Xiao[1] · Chao Huang[1] · Miao Wang[1] · Chaohui Gu[4] · Xiaoping Zhang[1] · Guosong Jiang[1]

Received: 3 August 2019 / Revised: 23 October 2019 / Accepted: 28 October 2019 / Published online: 8 November 2019

Abstract

Circular RNAs (circRNAs) have been increasingly indicated to be important participants in the development and progression of various malignant tumors. Our previous studies found that hundreds of circRNAs were aberrantly expressed in bladder cancer (BC) by high-throughput sequencing and we have confirmed that the downregulated circRNAs circHIPK3, circRNA BCRC-3, and circNR3C1 played inhibitory roles in BC progression. In this study, we focused on the upregulated circRNAs and identified a novel circular RNA, hsa_circ_0001361 (circ0001361), was expressed at high levels in BC tissues and cell lines based on RNA-Seq data and qRT-PCR analysis, and it was positively corelated with pathologic grade and muscle invasion. Moreover, Kaplan–Meier survival analysis implied that BC patients with high circ0001361 expression level had a poor overall survival. Functionally, circ0001361 promoted BC cell invasion and metastasis both in vitro and in vivo, but had no effect on cell cycle and proliferation. Mechanistically, RNA sequencing analysis indicated that MMP9 was upregulated in circ0001361-overexpressed BC cells, and MMP9 was verified to mediate circ0001361-induced cell migration and invasion. Furthermore, we demonstrated that circ0001361 could directly interact with miR-491-5p to upregulate MMP9 expression. Collectively, our findings indicate that circ0001361 plays oncogenic role in BC invasion and metastasis through targeting the miR-491-5p/MMP9 axis, and it might be a potential novel target for BC therapy.

Introduction

Bladder cancer (BC) is the most common malignant tumor in the urinary system [1], and the cancer incidence and mortality rates continue to rise in recent decades [2]. Approximately 25% of urothelial carcinomas are diagnosed as muscle invasive BC [3], which are associated with a worse prognosis because of half of the patients with muscle invasive BC develop distant metastases [4]. However, the exact mechanisms that regulate BC progression and metastasis remain unclear. Hence, further exploration of the biological and molecular mechanisms regulating invasion and metastasis of BC is crucial for improving the diagnosis and treatment of BC.

As a new member of non-coding RNA, circRNAs are a class of covalently closed RNA without a 5′ cap nor a 3′ polyadenylated tail [5–7]. Compared with linear RNA, circRNAs are more stable and not easily degraded by exonuclease [8]. CircRNAs were first discovered with electron microscope in 1979 and were initially considered as the products of precursor mRNA splicing errors with little functional potential [9, 10]. In recent years, with the

These authors contributed equally: Feng Liu, Hui Zhang, Fei Xie

Supplementary information The online version of this article (https://doi.org/10.1038/s41388-019-1092-z) contains supplementary material, which is available to authorized users.

✉ Xiaoping Zhang
xzhang@hust.edu.cn

✉ Guosong Jiang
jiangguosongdoc@hotmail.com

[1] Department of Urology, Union Hospital, Tongji Medical College, Huazhong University of Science and Technology, Wuhan 430022, China

[2] Department of Urology, The Affiliated Hospital of Qingdao University, Qingdao 266013, China

[3] Department of Oncology, The Fifth Hospital of Wuhan, Wuhan 430050, China

[4] Department of Urology, The First Affiliated Hospital of Zhengzhou University, Zhengzhou, Henan 450052, China

emergence of next-generation RNA sequencing (RNA-seq), circRNAs were discovered to be widely expressed in eukaryotes, indicating that they might have multiple roles in regulating gene expression [5, 11, 12]. Studies have revealed that circRNAs can be expressed in a tissue-specific or developmental stage-specific manner [8, 13, 14]. Importantly, emerging evidences have demonstrated that circRNAs are implicated in various human diseases, including heart failure [15], atherosclerotic [16], neurological disorders [17], and tumorigenesis [18]. CircRNAs harboring miRNA response elements can function as miRNA sponges to regulate the expression of downstream target genes. This notion has been supported by a series of previous studies. For example, circRNA CiRS-7 functioned as an effective miR-7 sponge to regulate miR-7 target mRNA expression [5], heart-related circRNA (HRCR) protected the heart from pathological hypertrophy and heart failure by sponging miR-223 [15], and circMTO1 suppressed hepatocellular carcinoma cell progression by acting as the sponge of oncogenic miR-9 to enhance p21 expression [19].

In recent years, the relationship between circRNAs and cancer has become a focused issue in the field of cancer research, and hundreds of circRNAs have been demonstrated to be aberrantly expressed in various human cancers [18–25], including BC. CircRNAs have been discovered to be associated with cellular proliferation, apoptosis, epithelial to mesenchymal transition (EMT), invasion, and metastasis of BC [20, 21, 23, 26]. Our previous studies have verified some downregulated circRNAs in the development and progression of BC, including circHIPK3 [14], circRNA BCRC-3 [20], and circNR3C1 [21]. Meanwhile, other studies have also found the crucial role of circRNAs in BC progression. For example, circRNA-MYLK has been discovered to promote BC occurrence and metastasis through VEGFA/VEGFAR2 signaling pathway [25], circTCF25 has been demonstrated to facilitate the proliferation and migration of BC by acting as miR-103a-3p/miR-107 sponge to increase the expression of CDK6 [27], and it showed that circPRMT5 could promote BC metastasis through sponging miR-30c to induce EMT [26]. However, the potential mechanisms and biological functions of most abnormally expressed circRNAs in BC remain unclear. Therefore, more dysregulated circRNAs still need to be clarified for investigating biological and molecular mechanisms associated with BC progression, which is expected to make a breakthrough in the clinical application for BC treatment.

In this study, we focused on the upregulated circRNAs based on our RNA-Seq data for the first time, and discovered that circ000136, which has not been reported previously, was upregulated in BC tissues and cell lines, and high expression of circ0001361 was positively associated with pathologic grade and muscle invasion. Importantly, we found that circ0001361 could directly sponge miR-491-5p to upregulate MMP9 expression and consequently enhance the invasion and metastasis of BC. Therefore, circ0001361 may serve as an oncogene to promote BC metastasis. Our study provides a novel therapeutic target for BC.

Results

Circ0001361 is upregulated in BC tissues and cell lines, and mainly distributes in the cytoplasm

Our previous studies discovered that hundreds of circRNAs were aberrantly expressed in BC using RNA-seq analysis of ribosomal RNA-depleted total RNA from three paired BC tissues and matched nontumorous tissues, and we have confirmed that the downregulated circRNAs circHIPK3 [14], circRNA BCRC-3 [20], and circNR3C1 [21] play inhibitory roles in BC progression. In this study, we focused on the upregulated circRNAs and screened the candidates according to the following criteria: (1) FC (fold change) ≥ 2 and $P < 0.05$; (2) read scores ≥2; (3) upregulated in each pair; (4) validated in circBase (http://www.circbase.org/) (Fig. 1a). Subsequently, circ0001361, which was significantly upregulated in BC tissues compared with paired normal tissues, was selected for further study. The genomic structure indicates that circ0001361 is composed of exons 2 and 3 of FNDC3B gene (GenBank: NM_022763). FNDC3B can produce a variety of different circRNAs. For example, circFNDC3B is derived from exons 5 and 6 of the FNDC3B gene [28]. Circ0001361 is a novel circRNA generated from FNDC3B, which has not been studied previously. Subsequently, the head-to-tail splicing of circ0001361 was further confirmed by Sanger sequencing (Fig. 1b). However, we cannot exclusive the possibilities that head-to-tail splicing might be the results of trans-splicing or genomic rearrangements [29]. In order to rule out these two possibilities, convergent primers and special divergent primers were designed to amplify FNDC3B mRNA and circ0001361, and both cDNA and gDNA extracted from T24T and UMUC3 cells were used as templates. The results indicated that circ0001361 could be amplified only in cDNA by divergent primers, but not in gDNA (Fig. 1c). Furthermore, we confirmed that circ0001361 was much more resistant to RNase R than linear FNDC3B mRNA (Fig. 1d, e).

Then, we evaluated the expression of circ0001361 in 69 cases of clinical BC tissues with different stages and their corresponding adjacent normal bladder mucosa tissues using qRT-PCR. A significant upregulation of circ0001361 expression was observed in BC tissues compared with their adjacent normal bladder tissues (Fig. 1f). Furthermore, upregulation of circ0001361 in BC patients was positively correlated with the clinical indicators including BC

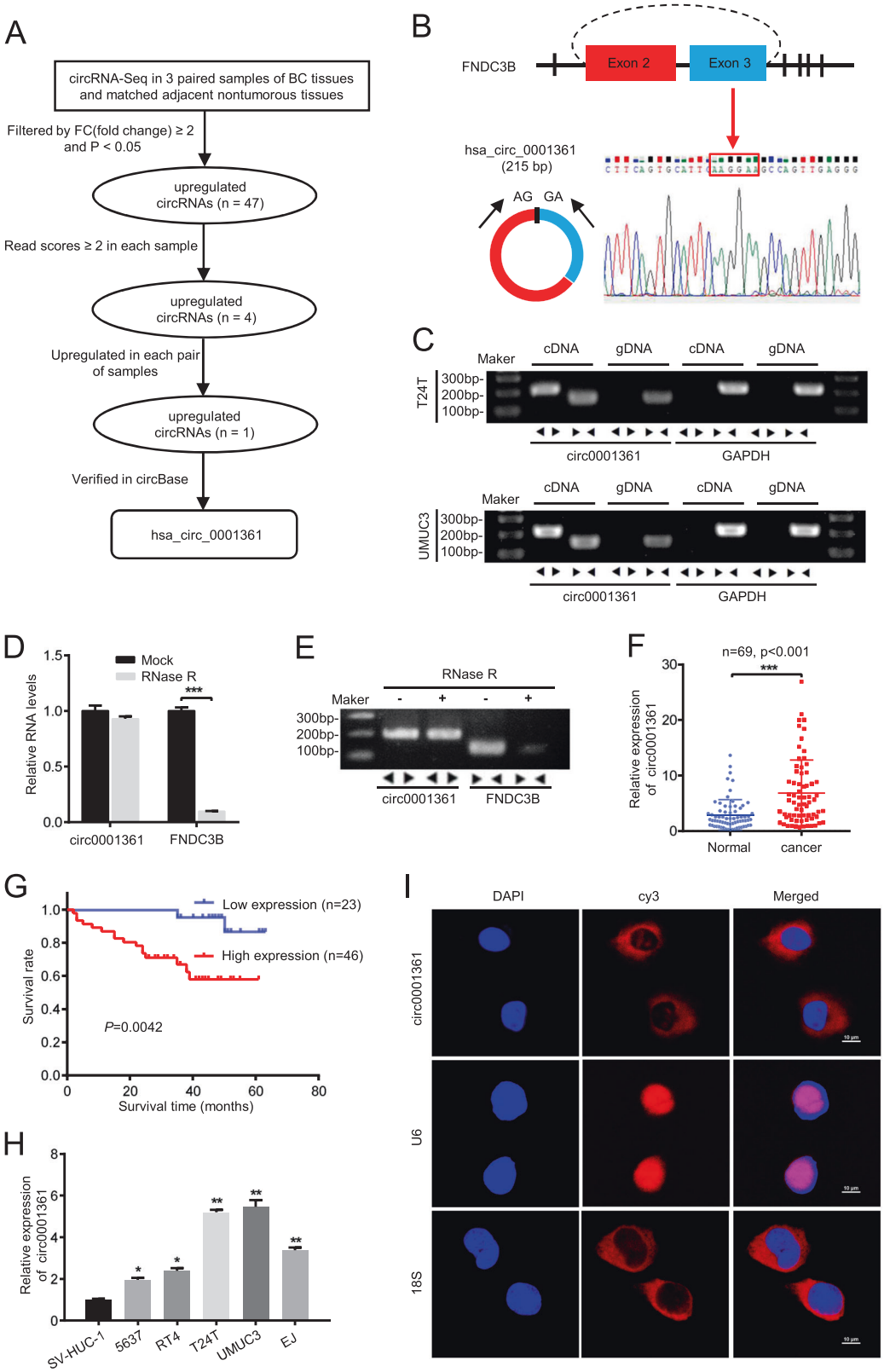

pathologic grade, clinical stage, vessel invasion and muscle invasion (Table 1). In addition, Kaplan–Meier survival analysis implied that BC patients with high circ0001361 expression level had a poor overall survival (OS) (Fig. 1g). Consistent with these findings, invasive BC cells lines (EJ, T24T, and UMUC3) showed significantly increased

◀ **Fig. 1** Circ0001361 is upregulated in BC tissues and cell lines, and mainly distributes in the cytoplasm. **a** Flowchart depicted the identification of circ0001361 as an upregulated circRNA in BC. **b** Schematic illustration showed the circularization of FNDC3B exon 2 and 3 formed circ0001361. The back-splice junction of circ0001361 was identified by Sanger sequencing. **c** As shown by agarose gel electrophoresis, circ0001361 could only be amplified with the divergent primers in cDNA, but not in gDNA. **d**, **e** The expression levels of circ0001361 and FNDC3B mRNA in UMUC3 cells were evaluated by RT-PCR or qRT-PCR detections of total RNA samples with or without (mock) RNase R treatment. **f** The expression level of circ0001361 in 69 paired of BC and corresponding adjacent tissues was determined by qRT-PCR. GAPDH was used as a loading control. **g** Kaplan–Meier's analyze of correlation between circ0001361 expression level and overall survival of 69 patients with BC ($n = 69$, $p = 0.0042$, log-rank test). **h** The expression level of circ0001361 in bladder noncancer cell line (SV-HUC-1) and cancer cell lines (RT4, 5637, EJ, T24T, and UMUC3) was detected by qRT-PCR. **i** RNA FISH images showed that circ0001361 was mainly distributed in the cytoplasm of UMUC3 (circ0001361, 18S and RNU6-1 probes were labeled with Cy3, the nuclei stained with DAPI). Scale bar, 10 μm. Data are presented as the means ± SEM of three independent experiments. $^{*}P < 0.05$; $^{**}P < 0.01$; $^{***}P < 0.001$ (Student's *t* test)

circ0001361 expression compared with superficial non-invasive BC cell lines (5637 and RT4) and normal urothelial epithelial cells (SV-HUC-1) (Fig. 1h). In order to further obtain the cell distribution of circ0001361, RNA fluorescence in situ hybridization (FISH) assay was conducted, and the results indicated that circ0001361 mainly localized in the cytoplasm (Fig. 1i).

Circ0001361 promotes invasion and metastasis of BC cells in vitro and in vivo

To explore the functions of circ0001361 in BC, vectors containing shRNA sequences specifically target the back-splicing region of circ0001361 were stably transfected into T24T and UMUC3 cells, and it was confirmed that circ0001361 expression was profoundly downregulated, while the linear FNDC3B mRNA level was not affected (Fig. 2a). The wound-healing assay revealed that silencing of circ0001361 significantly inhibited cell migration (Fig. 2b). Transwell migration and matrigel invasion assays further demonstrated that silencing of circ0001361 significantly suppressed BC cell migration and invasion (Fig. 2c). To further address the role of circ0001361 in BC, T24T, and UMUC3 cells with stable overexpression of circ0001361 were constructed (Fig. 2d). Consistently, transwell and wound-healing assays showed that stable overexpression of circ0001361 remarkably promoted BC cell migration and invasion (Fig. 2e, f). On the other hand, CCK8, EdU and cell cycle assays were performed, and the results demonstrated that knockdown or overexpression of circ0001361 in T24T and UMUC3 cells had no obvious effect on cell proliferation and cell cycle progression (Supplementary Fig. 1a–d).

To investigate the effects of circ0001361 on BC metastasis in vivo, we established a nude mouse lung metastasis model by tail vein injecting of circ0001361-knocked down UMUC3 cells. The tumor lung metastasis was monitored 7 weeks after tail vein injection of UMUC3 cells. Bioluminescence imaging and hematoxylin and eosin (H&E) staining showed that knockdown of circ0001361 significantly decreased the number of pulmonary metastasis focuses (Fig. 2g, h). Taken together, these results indicated that circ0001361 played an oncogenic role to promote invasion and metastasis in BC.

Circ0001361 facilitates BC cell invasion by targeting MMP9

We have discovered that circ0001361 especially promoted BC cell invasion and metastasis both in vitro and in vivo, but did not affect cell proliferation or cell cycle progression. Subsequently, transcriptome analysis was performed to find the downstream target that mediated circ0001361-induced cell invasion and metastasis in BC. A total of 16 mRNAs were upregulated and 50 mRNAs were downregulated in circ0001361-overexpressed T24T cells, while 57 mRNAs were upregulated and 32 mRNAs were downregulated in circ0001361-overexpressed UMUC3 cells (Supplementary Table 1 and Supplementary Fig. 2a, b). Among these differentially expressed mRNAs, only MMP9 was upregulated in both T24T and UMUC3 cells, whereas no consistently downregulated gene was observed (Fig. 3a, b). These results were further confirmed by qRT-PCR, which showed that the expression level of MMP9 mRNA was increased in circ0001361-overexpressed cells and decreased in circ0001361-silenced cells (Fig. 3c, d). Then, a series of key proteins associated with BC invasion including Heparanase (HPSE), MMP2, MMP9, E-cadherin, and Vimentin were detected by western blot. The results indicated that the protein level of MMP9 was significantly upregulated in circ0001361-overexpressed cells and downregulated in circ0001361-deficient cells, while the levels of other proteins did not change (Fig. 3e, f). To explore the effect of circ0001361 on MMP9 expression in vivo, we detected both mRNA and protein levels of MMP9 in lung metastatic nodules. The qRT-PCR results showed that the expression levels of circ0001361 and MMP9 were decreased in circ0001361-silenced group compared with the control group (Fig. 3g). Consistently, immunohistochemical (IHC) analysis showed that the expression of MMP9 protein in BC lung metastases was decreased by silencing of circ0001361 (Fig. 3h). To further address whether MMP9 was the major downstream effector of circ0001361, cell migration and invasion abilities were examined. It showed that overexpression of MMP9 could significantly rescue cell migration and invasion inhibition induced by circ0001361

Table 1 Clinicopathological features and expression of circ0001361 in 69 patients with bladder cancer

Variables	Group	Cases	Circ0001361 expression				*P* value
			Low	%	High	%	
Age at surgery	<60	18	8	44.4	10	55.6	0.2448
	≥60	51	15	29.4	36	70.6	
Gender	Male	54	16	29.6	38	70.4	0.2156
	Female	15	7	46.7	8	53.3	
pathological stage	pTa-T1	25	14	56.0	11	44.0	0.0026**
	pT2-T4	44	9	20.5	35	79.5	
Tumor sizes	<3.0 cm	27	8	29.6	19	70.4	0.6008
	≥3.0 cm	42	15	35.7	27	64.3	
Grade	Low	19	12	63.2	7	36.8	0.0012**
	High	50	11	22.0	39	78.0	
Blood vessel invasion	Absent	53	22	41.5	31	58.5	0.0204*
	Present	16	1	6.3	15	93.7	
Muscle invasion	NMIBC	25	14	56.0	11	44.0	0.0026**
	MIBC	44	9	20.5	35	79.5	
lymphatic metastasis	Absent	60	20	33.3	40	66.7	0.7046
	Present	9	3	33.3	6	66.7	
Total		69	23		46		

Chi-square test

*$P < 0.05$; **$P < 0.001$

knockdown (Fig. 4a). Meanwhile, qRT-PCR and western blot revealed that overexpression of MMP9 could significantly reverse the decrease of MMP9 expression caused by circ0001361 knockdown (Fig. 4b, c). Collectively, these results indicated that MMP9 mediated circ0001361-induced promotion of invasion and metastasis in BC.

Circ0001361 directly interacts with miR-491-5p in BC cells

To further clarify how circ0001361 promoted the expression of MMP9, 5′-UTR, promoter region, and 3′-UTR related luciferase reporters of MMP9 were respectively constructed. Dual-luciferase reporter assay showed that overexpression or knockdown of circ0001361 could increase or decrease the luciferase activity of MMP9 3′-UTR reporter, respectively, while the activities of MMP9 promoter and its 5′-UTR were not changed (Fig. 5a, b), which indicated that circ0001361 promoted MMP9 expression by enhancing MMP9 3′-UTR activity. Given the important role of miRNA in the regulation of mRNA 3′ UTR activity [30], TargetScan database was used to analyze the potential miRNA binding sites of MMP9 3′-UTR region and 60 miRNAs were predicted. It has been shown that circRNAs can function as miRNA sponges to regulate the expression of downstream genes [5, 31]. We next explored whether circ0001361, located in the cytoplasm, might function as miRNA sponge. RNAhybrid database was used to predict the potential circ0001361-targeted miRNAs and 155 miRNAs were selected from the database. Interestingly, among the 155 miRNAs, 4 miRNAs (miR-491-5p, miR-204-5p, miR-892b and miR-3691) were predicted to bind to MMP9 3′-UTR region (Fig. 5c).

To elucidate whether circ0001361 could directly bind these candidate miRNAs, RNA pull-down assay was conducted with specific biotin-labeled circ0001361 probe. The efficiency and specific of pull-down assay were verified by the results that circ0001361 could be specifically enriched by circ0001361 probe (Fig. 5d, e). Then, the relative levels of the four candidate miRNAs pulled down by circ0001361 were evaluated. We found that only miR-491-5p was abundantly pulled down in both T24T and UMUC3 cell lines, while miR-204-5p was slightly pulled down (Fig. 5f). Therefore, we chose miR-491-5p for further study. Two potential binding sites of miR-491-5p were identified in circ0001361 sequences ($\Delta G < -20$ kcal/mol) (Supplementary Fig. 3a, b). To define which binding site was functional, we separately mutated these two binding sites in circ0001361 overexpression vector and detected whether the mutants could still enrich miR-491-5p (Fig. 5g). The results showed that miR-491-5p pulled down by circ0001361 mutants was significantly decreased after mutation of binding site 1, or both site 1 and site 2, whereas this effect was not observed while only binding site 2 was mutated (Fig. 5h). These data indicated that binding site1 was essential for circ0001361 to sponge miR-491-5p. In order to further illustrate the direct interaction between miR-491-5p and circ0001361, biotinylated miR-491-5p

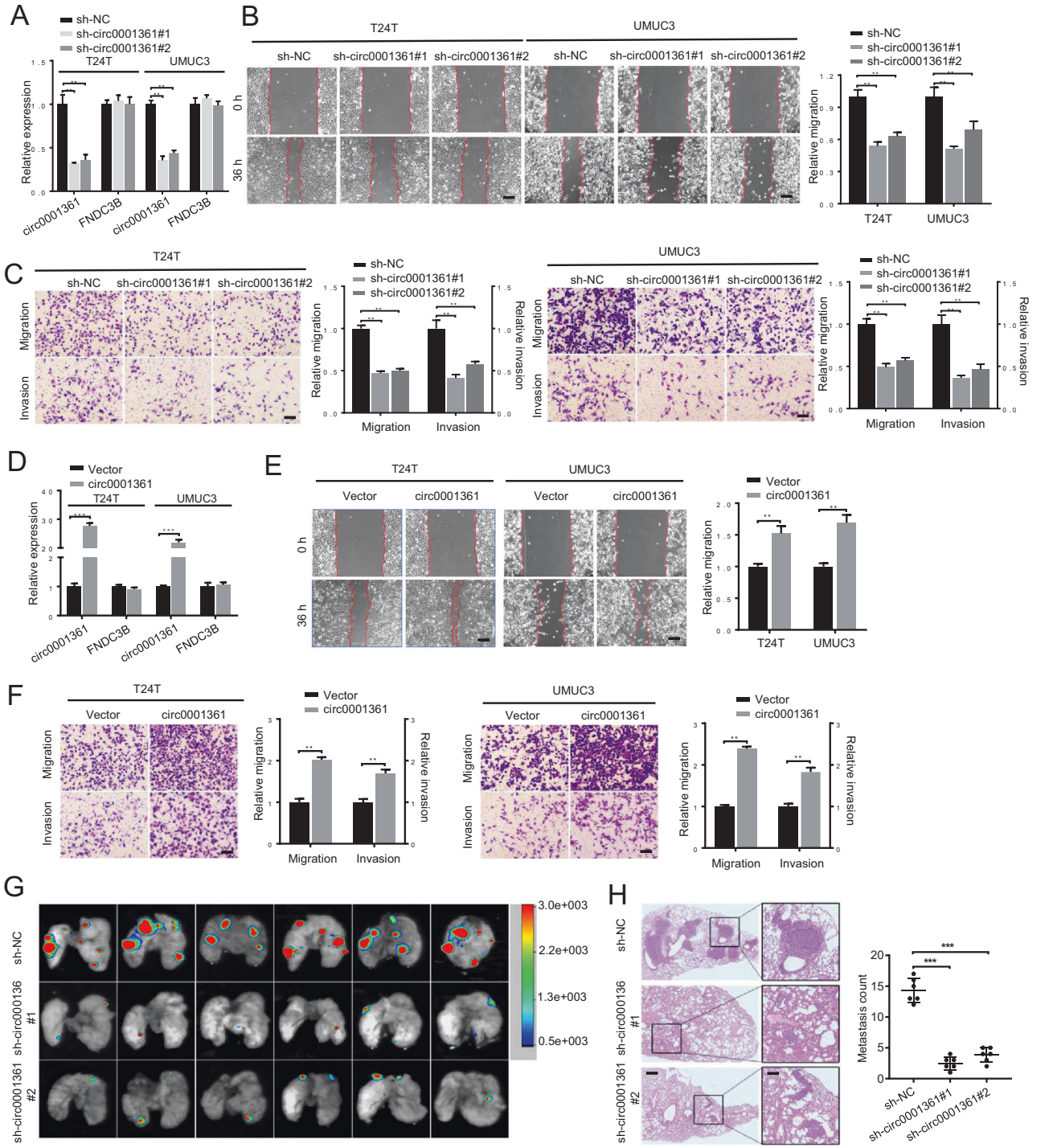

Fig. 2 Circ0001361 promotes invasion and metastasis of BC cells in vitro and in vivo. **a** The expression levels of circ0001361 and FNDC3B in T24T and UMUC3 cells stably transfected with sh-circ0001361 or corresponding negative control were detected by qRT-PCR. **b** The cell migration capability was evaluated by the wound-healing assay in circ0001361-silenced cells and corresponding control cells. Scale bar, 200 μm. **c** Silencing of circ0001361 inhibited cell migration and invasion capacities, as determined by transwell migration and matrigel invasion experiments. Scale bar, 100 μm. **d** The expression levels of circ0001361 and FNDC3B in T24T and UMUC3 cells after stable transfection of circ0001361 or vector plasmids were detected by qRT-PCR. **e** Overexpression of circ0001361 enhanced cell migration capacity, as determined by the wound-healing assay. Scale bar, 200 μm. **f** Cell migration and invasion abilities of T24T and UMUC3 cells stably transfected with vector or circ0001361 were evaluated by transwell migration and matrigel invasion assays. Scale bar, 100 μm. **g** Bioluminescence in vivo imaging showed that knockdown of circ0001361 significantly decreased the number of pulmonary metastasis focuses ($n = 6$ per group). **h** H&E staining showed that knockdown of circ0001361 led to decreased lung metastatic colonies. Scale bars, 100 and 200 μm. Data are presented as the means ± SEM of three independent experiments. $^{*}P < 0.05$; $^{**}P < 0.01$; $^{***}P < 0.001$ (Student's t test)

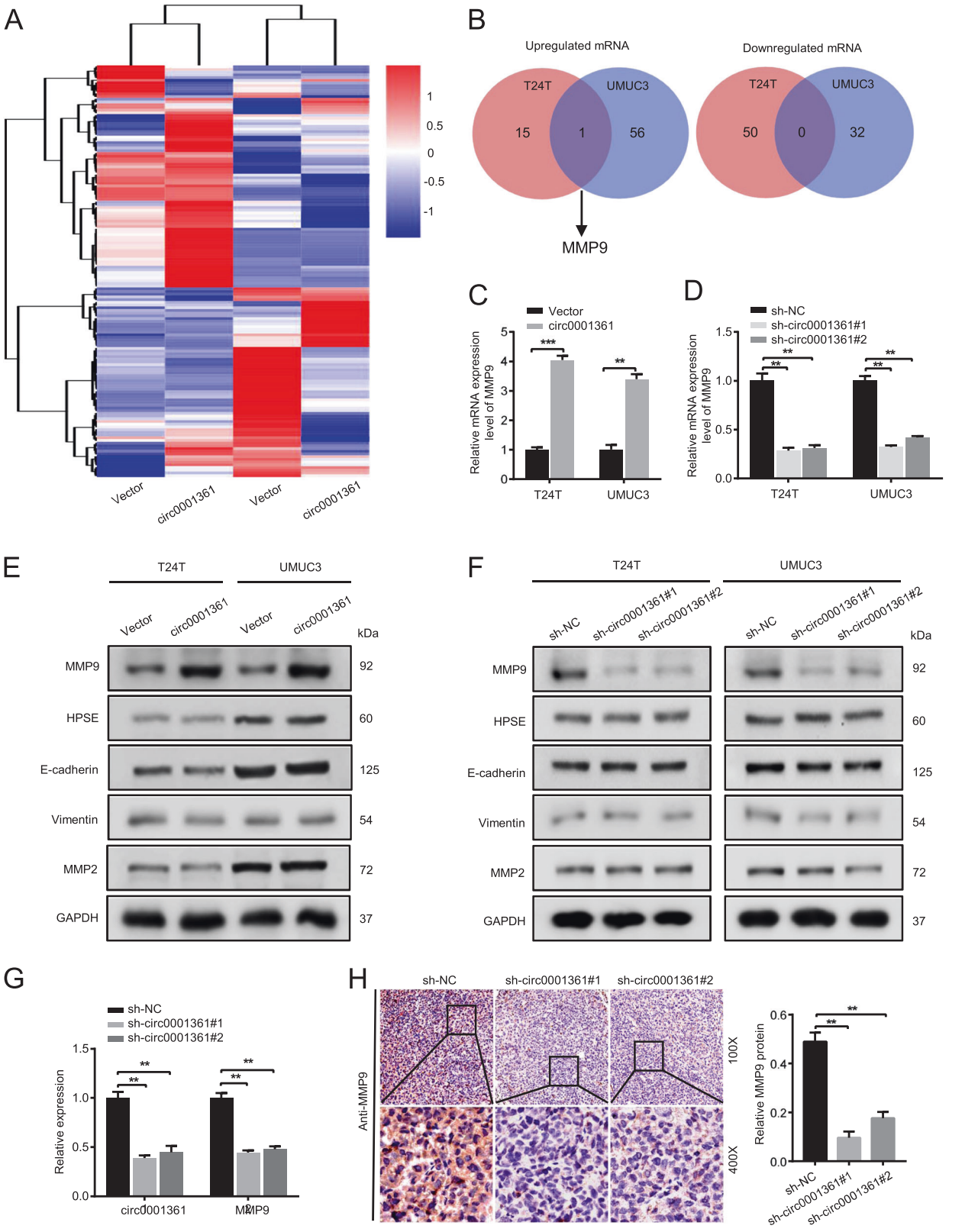

pull-down assay was performed. It showed that the enrichment of circ0001361 in miR-491-5p mutant-captured fraction was largely diminished compared with the wild-type miR-491-5p-captured fraction (Fig. 5i). On the other hand, we have also applied biotin-coupled miR-204-5p mimic pull-down assay and the results indicated that the

◀ **Fig. 3** Circ0001361 upregulates MMP9 expression. **a** Clustered heatmap of significant differentially expressed mRNAs in T24T and UMUC3 cells transfected with control vector or circ0001361 overexpression plasmid. Each sample contained a mixture of three repeats. **b** Schematic flowchart showed the overlapping of the upregulated and downregulated mRNAs collection in T24T and UMUC3 cells (filtered by fold change ≥ 2 or ≤−2 and *p*-value ≤ 0.05). **c**, **d** The mRNA level of MMP9 in BC cells with overexpression or knockdown of circ0001361 was determined by qRT-PCR. **e**, **f** The expression levels of MMP9, MMP2, HPSE, E-cadherin, and Vimentin in BC cells with overexpression or knockdown of circ0001361 were detected by western blot. **g** qRT-PCR analysis of circ0001361 and MMP9 expression levels in mice lung metastatic lesions. **h** Representative images of immunohistochemistry (IHC) detection of MMP9 in lung metastatic nodules. Protein expression levels were analyzed by the comprehensive optical density (IOD/area) of each staining area by image-pro Plus 6.0. Data are presented as the means ± SEM of three independent experiments. $^{**}P < 0.01$; $^{***}P < 0.001$ (Student's *t* test)

enrichment of circ0001361 did not change while miR-204-5p was mutated (Supplementary Fig. 4a–c), suggesting that miR-491-5p, but not miR-204-5p, was the major direct target of circ0001361. In addition, RNA FISH detection indicated that circ0001361 and miR-491-5p were co-localized in the cytoplasm (Fig. 5j). Collectively, these results demonstrated that circ0001361 could directly interact with miR-491-5p in BC cells.

Circ0001361 sponges miR-491-5p to upregulate MMP9 expression and promote cell invasion in BC

Next, we explore the role of interaction between circ0001361 and miR-491-5p in regulation of MMP9 expression and cell invasion. Firstly, we detected the

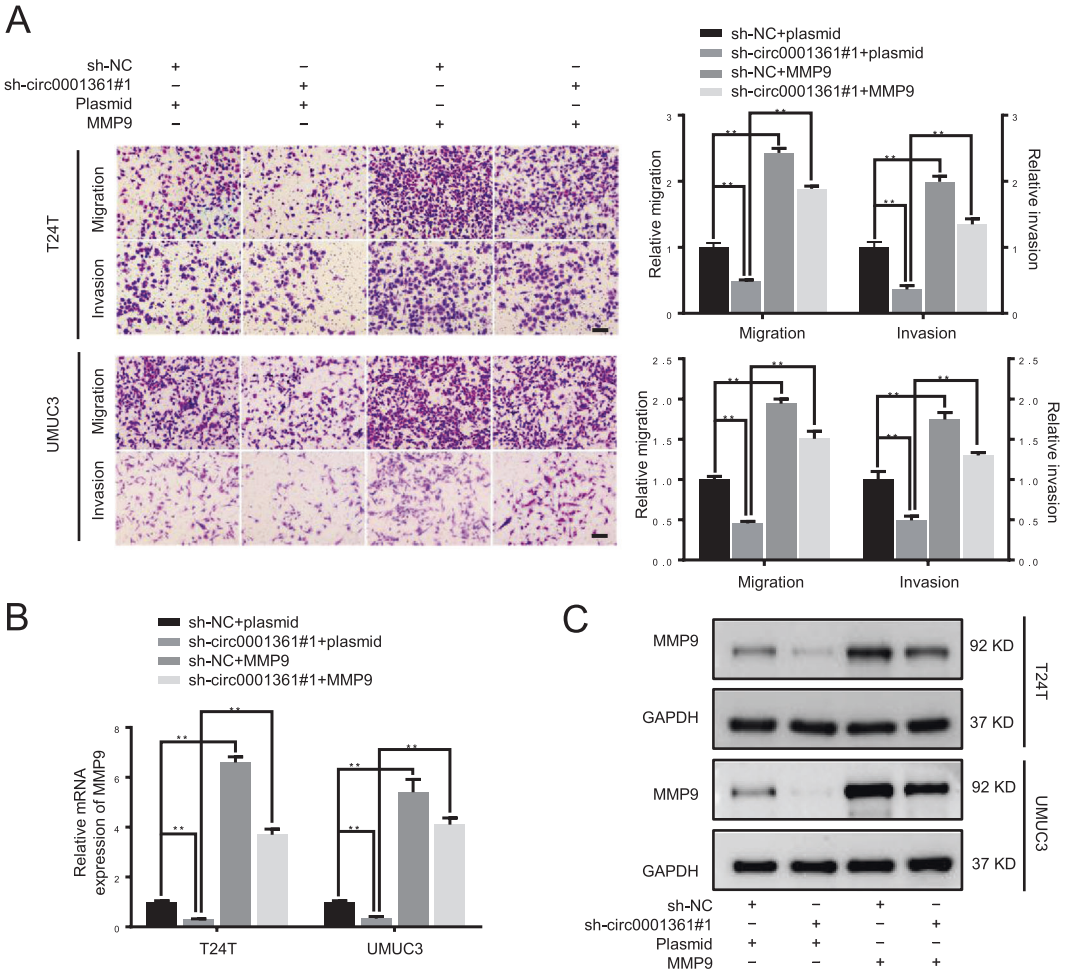

Fig. 4 Circ0001361 facilitates BC cell invasion through targeting MMP9. **a** Representative images and quantification results of transwell migration and matrigel invasion assays for T24T and UMUC3 cells upon circ0001361 knockdown combined with MMP9 overexpression. Scale bar, 100 μm. **b**, **c** qRT-PCR and western blot were performed to evaluate the expression of MMP9 in T24T and UMUC3 cells which were transfected with the indicated plasmids. GAPDH was used as internal control. The results were derived from three independent experiments. Data are presented as the means ± SEM of three independent experiments. $^{*}P < 0.05$; $^{**}P < 0.01$ (Student's *t*-test)

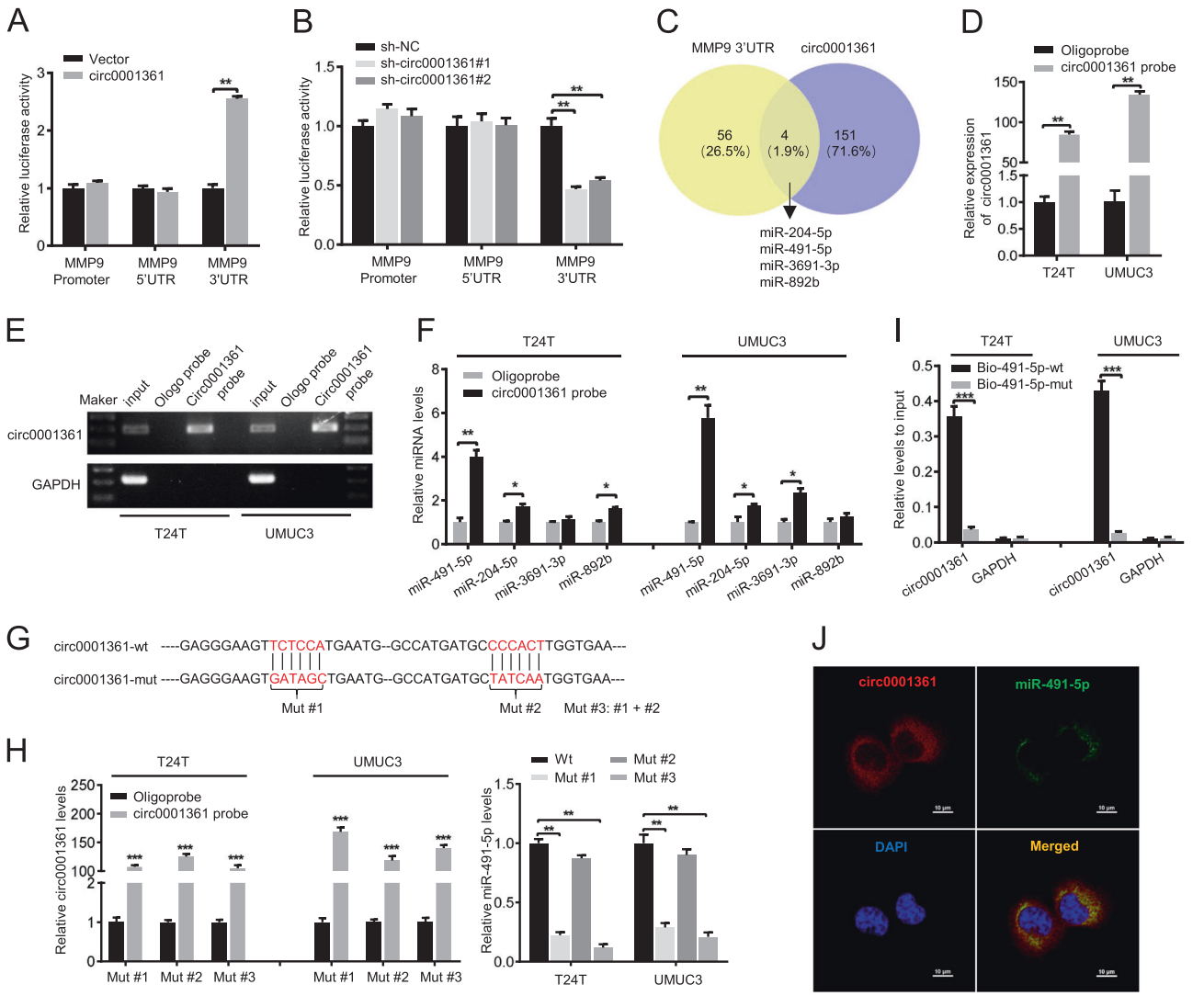

Fig. 5 Circ0001361 directly interacts with miR-491-5p in BC cells. **a**, **b** The promoter, 5′UTR and 3′UTR of MMP9 luciferase activities were measured after overexpression or knockdown of circ0001361 in UMUC3 cells. **c** Schematic illustration showed the overlapping of the target miRNAs of MMP9 3′UTR and circ0001361 predicted by TargetScan and RNAhybrid. **d**, **e** qRT-PCR and gel electrophoretic results showed that circ0001361 could be specifically enriched by circ0001361 probe. Relative level of circ0001361 was normalized to input. GAPDH was used as negative control. **f** The relative expression levels of four miRNAs candidates were detected by qRT-PCR in T24T and UMUC3 cell lysates. **g** Schematic graph illustrated the mutants of potential binding sites between miR-491-5p and circ0001361. Mut #1 and Mut #2, respectively, represented the potential binding site 1 and 2 was mutated, and Mut #3 represented both potential binding sites were mutated. **h** The relative levels of circ0001361 mutants and miR-491-5p pulled down by circ0001361 probe in cell lysates were tested by qRT-PCR. **i** Circ0001361 was enriched by biotinylated wild-type miR-491-5p (Bio-491-5p-wt) or its mutant (Bio-491-5p-mut), and qRT-PCR was used to determine the relative circ0001361 and GAPDH mRNA levels. **j** RNA FISH images showed the co-localization of circ0001361 and miR-491-5p in the cytoplasm of UMUC3 cells (circ0001361 probe was labeled with Cy3, locked nucleic acid miR-491-5p was labeled with Dig, and the nuclei were stained with DAPI). Scale bar, 10 μm. Data are presented as the means ± SEM of three independent experiments. $*P < 0.05$; $**P < 0.01$; $***P < 0.001$ (Student's t test)

expression level of miR-491-5p in 69 pairs of BC tissues and matched noncancer tissues and found that the expression level of miR-491-5p in BC tissues was significantly decreased (Fig. 6a). Consistently, miR-491-5p was also obviously downregulated in EJ, T24T, and UMUC3 cells compared with SV-HUC-1 cells (Fig. 6b). However, overexpression or knockdown of circ0001361 did not affect the expression of miR-491-5p in T24T and UMUC3 cells (Supplementary Fig. 5a, b). Pearson correlation analysis also displayed no significant correlation between circ0001361 expression and miR-491-5p expression in the 69 paired samples of BC (Supplementary Fig. 5c). These results suggested that the low expression of miR-491-5p was not regulated by circ0001361 in BC.

Next, we evaluated the effect of miR-491-5p on MMP9 expression. The results showed that miR-491-5p mimics

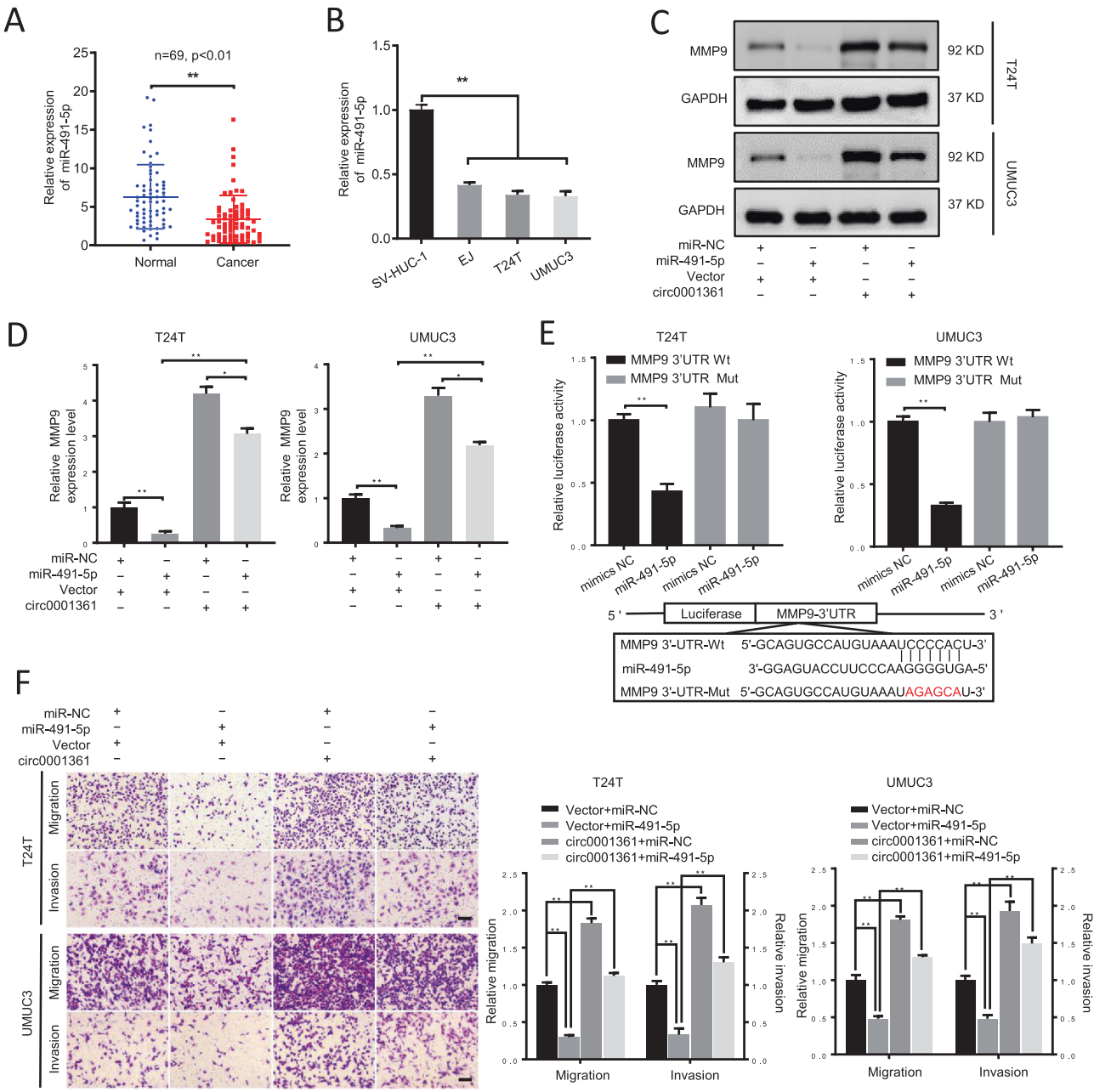

Fig. 6 Circ0001361 sponges miR-491-5p to upregulate MMP9 expression and promote cell invasion in BC. **a**, **b** qRT-PCR results showed that miR-491-5p was decreased in both BC tissues ($n = 69$) and cell lines compared with corresponding para-cancer normal tissues and SV-HUC-1 cells. **c**, **d** MMP9 expression level in T24T and UMUC3 cells transfected with miR-491-5p mimics alone or co-transfected with circ0001361 was determined by western blot and qRT-PCR. **e** Upper panel: The relative luciferase activities of wild type MMP9 3′UTR and its mutant after transfected with miR-491-5p mimic in T24T and UMUC3 cells. Lower panel: Schematic graph illustrated the mutation of potential binding site between miR-491-5p and the 3′-UTR regions of MMP9. **f** Representative images and quantification results of transwell migration and matrigel invasion assay for T24T and UMUC3 transfected with miR-491-5p mimics alone or co-transfected with circ0001361. Scale bar, 100 μm. Data are presented as the means ± SEM of three independent experiments. $^{*}P < 0.05$; $^{**}P < 0.01$ (Student's t test)

significantly decreased MMP9 mRNA and protein levels, which could be reversed by circ0001361 overexpression (Fig. 6c, d). Subsequently, to clarify how MMP9 was regulated by miR-491-5p, luciferase reporters containing wild type and mutated putative binding sites of MMP9 3′ UTR transcript were constructed (Fig. 6e, lower panel and Supplementary Fig. 3c). Dual-luciferase reporter assay showed that the luciferase activity of wild type MMP9 3′ UTR reporter was significantly decreased when the BC cells were transfected with miR-491-5p mimics, whereas this effect was not observed in the mutated MMP9 3′UTR (Fig. 6e, upper panel), indicating that miR-491-5p could

directly bind to MMP9 3′UTR region with an inhibitory effect on its activity. Transwell migration and invasion assays further indicated that enforced expression of miR-491-5p significantly inhibited BC cell migration and invasion, and these inhibitory effects could be partly reversed by circ0001361 overexpression (Fig. 6f). Taken together, these results revealed that circ0001361 acted as a sponge for miR-491-5p to upregulate MMP9 expression and promote cell invasion in BC.

Discussion

Increasing evidences show that circRNAs play an important role in the occurrence and development of cancers [32, 33]. Previously, we have found 524 significantly downregulated and 47 upregulated circRNAs in BC tissues by high-throughput sequencing. In the following studies, we have reported that circHIPK3 inhibited BC cell invasion by sponging miR-558 and suppressing HPSE expression [14], circRNA BCRC-3 suppressed BC cell proliferation through increasing p27 expression [20], and circNR3C1 sponged miR-27a-3p and downregulated cyclinD1 expression to impair BC cell proliferation [21]. However, the role of the upregulated circRNAs remains unclear. In this study, we found that circ0001361 was upregulated in BC tissues and cell lines. In vitro and in vivo studies showed that circ0001361 promoted BC cell invasion and metastasis. These results revealed that circ0001361 might play an oncogenic role in BC, and could be applied as a potential novel target for BC therapy in future. On the other hand, it was observed that circ0001361 expression was positively correlated with BC pathological grade and muscle invasion, and patients with high expression of circ0001361 tended to have significantly shorter survival time. It has been generally acknowledged that, compared with linear mRNA, circRNA is more stable and easier to detect in cells, plasma and even circulating exosomes [34, 35]. Thus, circ0001361 could possibly be used for potential diagnosis and prognosis evaluation of BC, which need to be further validated.

CircRNAs have been suggested to function as miRNA sponges with following characteristics: (1) derived from protein encoding exons; (2) mainly distributed in cytoplasm [36]. Given that circ0001361 derives from two exons of FNDC3B gene and mainly locates in the cytoplasm, we have demonstrated that circ0001361 acts as miRNA sponge to regulate downstream target gene. Previously, studies indicated that circRNAs, functioned as miRNA sponges, required multiple binding sites for the same miRNA, such as ciRS-7, Sry circRNA, and HRCR [5, 15]. In the present study, we found that circ0001361 contained two miR-491-5p binding sites, and further confirmed that only one of the binding sites was effective. Similarly, recent studies also showed that a lot of circRNAs only contained one or two binding sites for certain miRNAs, and could act as efficient miRNA sponges, such as circIRAK3 [37], circFNDC3B [28], circ101555 [38], and circTP63 [39]. Hence, we propose that circRNA may not require multiple binding sites for the same miRNA to function as miRNA sponge, and even one effective binding site is sufficient. Nevertheless, whether circ0001361 involves in other biological processes, such as binding RNA-binding proteins [22, 40, 41] or translating peptides [42, 43], still requires further investigation.

The abnormal expression of miRNAs in many human cancers plays important roles in tumorigenesis, development, and metastasis [44, 45]. MiR-491-5p has been reported to act as a tumor suppressor in multiple types of cancers [46–49], including oral squamous cell carcinoma, gastric cancer, prostate cancer and breast cancer. However, the role of miR-491-5p in BC has not been elucidated. In this study, we found that overexpression of miR-491-5p could inhibit BC cell migration and invasion, suggesting that miR-491-5p functioned as a tumor suppressor in BC. MMP9, an important oncogene, belongs to the zinc-dependent endopeptidase family, can degrade extracellular matrix and plays a vital role in tumorigenesis and metastasis [50]. Moreover, previous study indicated that MMP9 was closely associated with the development of invasive BC [51, 52]. It has been reported that miR-491-5p can inhibit invasion of gastric, breast and lung cancer cell lines via targeting MMP9 mRNA 3′UTR [53]. In this study, we have confirmed that miR-491-5p/MMP9 axis is critical for circ0001361-mediated oncogenic function in BC. Our study provides further evidences for the posttranscriptional regulation of MMP9 by circRNA and miRNA in BC cells. Previous studies have identified that miRNA biogenesis is regulated at multiple levels, including at the level of miRNA transcription, genetic alterations, and post-transcriptional regulation [54]. Interestingly, miR-491-5p's host gene, KIAA1797/FOCAD, has been reported to act as a tumor suppressor gene in glioma [55] and colorectal cancer [56], suggesting that the downregulation of miR-491-5p might correlated with the inhibition of its host gene. Nevertheless, the exact regulatory mechanisms still need to be explored in future studies.

In conclusion, our study found that the novel circRNA circ0001361 was upregulated in BC tissues and was positively correlated with pathologic grade, as well as muscle invasion of BC. Importantly, higher circ0001361 expression was significantly associated with poor OS rate in BC patients. Functionally, circ0001361 promoted BC cell invasion and metastasis both in vitro and in vivo. Mechanistically, circ0001361 increased MMP9 expression via acting as miR-491-5p sponge. Taken together, our study

clarified that circ0001361 acted as an oncogenic circRNA through targeting miR-491-5p/MMP9 axis, and provided a new target for the diagnosis and treatment of BC.

Materials and methods

The detailed procedures of siRNA synthesis, interference and overexpression vector construction, cell transfection, RT-PCR, qRT-PCR, RNase R treatment, wound-healing and transwell assays, cell viability assay, 5-Ethynyl-2′-deoxyuridine (EdU) assay, cell cycle assay, RNA FISH, western blotting, immunohistochemistry, oligo pull-down assay, and bioinformatics analysis are described in Supplementary Materials and methods.

Tissue of BC patients

A total of 69 pairs of BC tissues and matched adjacent normal bladder epithelial tissues (with a distance of ≥3 cm from the edge of cancer tissues) were obtained from BC patients who underwent radical cystectomy at Union Hospital of Tongji Medical College of Huazhong University of Science and Technology (Wuhan, China) from January 2014 to February 2017. None of the patients received chemotherapy or radiotherapy before surgery. All the specimens were identified by at least two experienced clinical pathologists independently according to the criteria of the sixth edition TNM classification of the International Union Against Cancer. These tissues were immediately frozen in liquid nitrogen, and then stored at −80 °C. The clinical information of the patients and the pathological features of all BC tissue specimens are listed in Table 1. We got the permission of the Institutional Review Board of Tongji Medical College of Huazhong University of Science and Technology and signed the informed consent with all patients before the research started.

Cell lines and cell culture

Human BC cell lines EJ, UMUC3, RT4, 5637, and human immortalized uroepithelium cell line (SV-HUC-1) were obtained from American Type Culture Collection (ATCC, USA). The human BC cell line T24T was provided by Dr Dan Theodorescu (Departments of Urology, University of Virginia) as described previously [14]. SV-HUC-1 cells were cultured in F-12 K medium (Gibco, USA), T24T and UMUC3 cells were cultured in Dulbecco's modified Eagle's medium (Thermo Scientific, USA), and 5637, EJ and RT4 cells were cultured in RPMI-1640 medium (Gibco, USA) supplemented with 10% FBS (Gibco, USA) and 1% penicillin/streptomycin (Gibco, USA) in an incubator at 37 °C with humidified atmosphere of 5% CO2. All cell lines were confirmed 4–6 months before use by using a short tandem repeat method and were tested negative for mycoplasma contamination.

UID (unique identifier) RNA sequencing

The gene expression profiles of circ0001361-overexpressed T24T and UMUC3 cells and the corresponding control cells were determined by UID-RNA-seq (SeqHealth Tech, China). Significant differentially expressed transcripts were screened by FC ≥ 2 or ≤ −2 and p-value ≤ 0.05 (Supplementary Table 1). The UID-RNA-seq data were deposited at the NCBI Gene Expression Omnibus database (https://www.ncbi.nlm.nih.gov/geo/query/acc.cgi?acc=GSE136919) with accession number GSE136919.

Animal studies

The animal studies were carried out in accordance with NIH Guidelines for the Care and Use of Laboratory Animals and approved by the Animal Care Committee of Tongji Medical College (approval number: 20182163). For the in vivo tumor metastasis studies, 4-week-old male BALB/c nude mice were randomly divided into three groups ($n = 6$ per group). UMUC3 cells that stably transfected with circ0001361 knockdown plasmid or negative control plasmid were injected into the nude mice via tail vein (2×10^6 cells per mouse), respectively. Seven weeks after tail vein injection, all the mice were sacrificed. For animal studies, no blinding was done. The In-Vivo FX PRO (BRUKER Corporation, USA) was used to obtain fluorescence images of xenografts in nude mice.

Dual-luciferase reporter assay

T24T and UMUC3 cells were seeded in 24-well plate (6×10^4 cells per well) 24 h before transfection. The pGL3-basic MMP9 promoter/5′-UTR and renilla luciferase reporter vectors (pRL-TK) were co-transfected with circ0001361 overexpression plasmid/shRNA plasmids, respectively, to examine the promoter and 5′-UTR activities of MMP9. Meanwhile, the psiCHECK2 MMP9 3′-UTR reporter vector were co-transfected with circ0001361 overexpression plasmid/shRNA plasmids to determine the 3′-UTR activity of MMP9. On the other hand, the cells were co-transfected with psiCHECK2 MMP9 3′-UTR-wide type/mutant reporter vector and miR-491-5p mimics (20 nM) to examine the miRNA binding abilities. After transfection for 48 h, the firefly and Renilla luciferase activities were measured with Dual-Luciferase® Reporter Assay System (Promega, USA) according to the manufacturer's protocol. The details of primers are listed in Supplementary Table 2.

Statistical analysis

All the data statistical analyses were performed using GraphPad Prism 7.0 software (La Jolla, USA), and were indicated as means ± standard error of the mean (SEM). Comparison between two groups was performed with two-tailed Student's *t* test. The relationship between circ0001361 expression and clinicopathologic characteristics was explored by chi-squared test. Correlation between circ0001361 and miR-491-5p expression was analyzed by Pearson's correlation. Kaplan–Meier survival curve and log-rank test were employed to depict the OS distributions of BC patients with different expression levels of circ0001361. One-way analysis of variance was performed to evaluate the group difference. $P < 0.05$ was considered statistically significant.

Acknowledgements This work was supported by the National Natural Science Foundation of China (Nos. 81672529, 81772724, 81874091, 81602234, 81702524).

Compliance with ethical standards

Conflict of interest The authors declare that they have no conflict of interest.

References

1. Antoni S, Ferlay J, Soerjomataram I, Znaor A, Jemal A, Bray F. Bladder cancer incidence and mortality: a global overview and recent trends. Eur Urol. 2017;71:96–108.
2. Bray F, Ferlay J, Soerjomataram I, Siegel RL, Torre LA, Jemal A. Global cancer statistics 2018: GLOBOCAN estimates of incidence and mortality worldwide for 36 cancers in 185 countries. CA Cancer J Clin. 2018;68:5–31.
3. Kamat AM, Hahn NM, Efstathiou JA, Lerner SP, Malmström PU, Choi W, et al. Bladder cancer. Lancet. 2016;388:2796–810.
4. Alfred Witjes J, Lebret T, Compérat EM, Cowan NC, De Santis M, Bruins HM, et al. Updated 2016 EAU guidelines on muscle-invasive and metastatic bladder cancer. Eur Urol. 2017;71:462–75.
5. Hansen TB, Jensen TI, Clausen BH, Bramsen JB, Finsen B, Damgaard CK, et al. Natural RNA circles function as efficient microRNA sponges. Nature. 2013;495:384–8.
6. Tay Y, Rinn J, Pandolfi PP. The multilayered complexity of ceRNA crosstalk and competition. Nature. 2014;505:344–52.
7. Guo JU, Agarwal V, Guo H, Bartel DP. Expanded identification and characterization of mammalian circular RNAs. Genome Biol. 2014;15:409.
8. Barrett SP, Salzman J. Circular RNAs: analysis, expression and potential functions. Development. 2016;143:1838–47.
9. Hsu MT, Coca-Prados M. Electron microscopic evidence for the circular form of RNA in the cytoplasm of eukaryotic cells. Nature. 1979;280:339–40.
10. Nigro JM, Cho KR, Fearon ER, Kern SE, Ruppert JM, Oliner JD, et al. Scrambled exons. Cell. 1991;64:607–13.
11. Memczak S, Jens M, Elefsinioti A, Torti F, Krueger J, Rybak A, et al. Circular RNAs are a large class of animal RNAs with regulatory potency. Nature. 2013;495:333–8.
12. Rybak-Wolf A, Stottmeister C, Glažar P, Jens M, Pino N, Giusti S, et al. Circular RNAs in the mammalian brain are highly abundant, conserved, and dynamically expressed. Mol Cell. 2015;58:870–85.
13. Jeck WR, Sorrentino JA, Wang K, Slevin MK, Burd CE, Liu J, et al. Circular RNAs are abundant, conserved, and associated with ALU repeats. RNA. 2013;19:141–57.
14. Li Y, Zheng F, Xiao X, Xie F, Tao D, Huang C, et al. CircHIPK3 sponges miR-558 to suppress heparanase expression in bladder cancer cells. Embo Rep. 2017;18:1646–59.
15. Wang K, Long B, Liu F, Wang J, Liu C, Zhao B, et al. A circular RNA protects the heart from pathological hypertrophy and heart failure by targeting miR-223. Eur Heart J. 2016;37:2602–11.
16. Burd CE, Jeck WR, Liu Y, Sanoff HK, Wang Z, Sharpless NE. Expression of linear and novel circular forms of an INK4/ARF-associated non-coding RNA correlates with atherosclerosis risk. PLoS Genet. 2010;6:e1001233.
17. Errichelli L, Dini Modigliani S, Laneve P, Colantoni A, Legnini I, Capauto D, et al. FUS affects circular RNA expression in murine embryonic stem cell-derived motor neurons. Nat Commun. 2017;8:14741.
18. Kristensen LS, Hansen TB, Veno MT, Kjems J. Circular RNAs in cancer: opportunities and challenges in the field. Oncogene. 2018;37:555–65.
19. Han D, Li J, Wang H, Su X, Hou J, Gu Y, et al. Circular RNA circMTO1 acts as the sponge of microRNA-9 to suppress hepatocellular carcinoma progression. Hepatology. 2017;66:1151–64.
20. Xie F, Li Y, Wang M, Huang C, Tao D, Zheng F, et al. Circular RNA BCRC-3 suppresses bladder cancer proliferation through miR-182-5p/p27 axis. Mol Cancer. 2018;17:144.
21. Zheng F, Wang M, Li Y, Huang C, Tao D, Xie F, et al. CircNR3C1 inhibits proliferation of bladder cancer cells by sponging miR-27a-3p and downregulating cyclin D1 expression. Cancer Lett. 2019;460:139–51.
22. Du WW, Fang L, Yang W, Wu N, Awan FM, Yang Z, et al. Induction of tumor apoptosis through a circular RNA enhancing Foxo3 activity. Cell Death Differ. 2017;24:357–70.
23. Yang C, Yuan W, Yang X, Li P, Wang J, Han J, et al. Circular RNA circ-ITCH inhibits bladder cancer progression by sponging miR-17/miR-224 and regulating p21, PTEN expression. Mol Cancer. 2018;17:19.
24. Liu H, Chen D, Bi J, Han J, Yang M, Dong W, et al. Circular RNA circUBXN7 represses cell growth and invasion by sponging miR-1247-3p to enhance B4GALT3 expression in bladder cancer. Aging. 2018;10:2606–23.
25. Zhong Z, Huang M, Lv M, He Y, Duan C, Zhang L, et al. Circular RNA MYLK as a competing endogenous RNA promotes bladder cancer progression through modulating VEGFA/VEGFR2 signaling pathway. Cancer Lett. 2017;403:305–17.
26. Chen X, Chen R, Wei W, Li Y, Feng Z, Tan L, et al. PRMT5 circular RNA promotes metastasis of urothelial carcinoma of the bladder through sponging miR-30c to induce epithelial-mesenchymal transition. Clin Cancer Res. 2018;24:6319–30.
27. Zhong Z, Lv M, Chen J. Screening differential circular RNA expression profiles reveals the regulatory role of circTCF25-miR-103a-3p/miR-107-CDK6 pathway in bladder carcinoma. Sci Rep. 2016;6:30919.
28. Liu H, Bi J, Dong W, Yang M, Shi J, Jiang N, et al. Invasion-related circular RNA circFNDC3B inhibits bladder cancer progression through the miR-1178-3p/G3BP2/SRC/FAK axis. Mol Cancer. 2018;17:161.
29. Jeck WR, Sharpless NE. Detecting and characterizing circular RNAs. Nat Biotechnol. 2014;32:453–61.

30. Bracken CP, Scott HS, Goodall GJ. A network-biology perspective of microRNA function and dysfunction in cancer. Nat Rev Genet. 2016;17:719–32.
31. Qu S, Yang X, Li X, Wang J, Gao Y, Shang R, et al. Circular RNA: a new star of noncoding RNAs. Cancer Lett. 2015;365:141–8.
32. Vo JN, Cieslik M, Zhang Y, Shukla S, Xiao L, Zhang Y, et al. The Landscape of circular RNA in cancer. Cell 2019;176:869–81.
33. Zhong Y, Du Y, Yang X, Mo Y, Fan C, Xiong F, et al. Circular RNAs function as ceRNAs to regulate and control human cancer progression. Mol Cancer. 2018;17:79.
34. Li Y, Zheng Q, Bao C, Li S, Guo W, Zhao J, et al. Circular RNA is enriched and stable in exosomes: a promising biomarker for cancer diagnosis. Cell Res. 2015;25:981–4.
35. Li Z, Huang C, Bao C, Chen L, Lin M, Wang X, et al. Exon-intron circular RNAs regulate transcription in the nucleus. Nat Struct Mol Biol. 2015;22:256–64.
36. Arnaiz E, Sole C, Manterola L, Iparraguirre L, Otaegui D, Lawrie CH. CircRNAs and cancer: biomarkers and master regulators. Semin Cancer Biol. 2019;58:90–9.
37. Wu J, Jiang Z, Chen C, Hu Q, Fu Z, Chen J, et al. CircIRAK3 sponges miR-3607 to facilitate breast cancer metastasis. Cancer Lett. 2018;430:179–92.
38. Chen Z, Ren R, Wan D, Wang Y, Xue X, Jiang M, et al. Hsa_circ_101555 functions as a competing endogenous RNA of miR-597-5p to promote colorectal cancer progression. Oncogene. 2019;38:6017–34.
39. Cheng Z, Yu C, Cui S, Wang H, Jin H, Wang C, et al. circTP63 functions as a ceRNA to promote lung squamous cell carcinoma progression by upregulating FOXM1. Nat Commun. 2019;10:3200.
40. Abdelmohsen K, Panda AC, Munk R, Grammatikakis I, Dudekula DB, De S, et al. Identification of HuR target circular RNAs uncovers suppression of PABPN1 translation by CircPABPN1. RNA Biol. 2017;14:361–9.
41. Ashwal-Fluss R, Meyer M, Pamudurti NR, Ivanov A, Bartok O, Hanan M, et al. circRNA biogenesis competes with pre-mRNA splicing. Mol Cell. 2014;56:55–66.
42. Yang Y, Gao X, Zhang M, Yan S, Sun C, Xiao F, et al. Novel role of FBXW7 circular RNA in repressing glioma tumorigenesis. JNCI. 2018;110:304–15.
43. Gu C, Zhou N, Wang Z, Li G, Kou Y, Yu S, et al. circGprc5a promoted bladder oncogenesis and metastasis through Gprc5a-targeting peptide. Mol Ther Nucleic Acids. 2018;13:633–41.
44. Nelson KM, Weiss GJ. MicroRNAs and cancer: past, present, and potential future. Mol Cancer Ther. 2008;7:3655–60.
45. Berindan-Neagoe I, Monroig PDC, Pasculli B, Calin GA. MicroRNAome genome: a treasure for cancer diagnosis and therapy. CA. 2014;64:311–36.
46. Hui Z, Yiling C, Wenting Y, XuQun H, ChuanYi Z, Hui L. miR-491-5p functions as a tumor suppressor by targeting JMJD2B in ERalpha-positive breast cancer. Febs Lett. 2015;589:812–21.
47. Huang WC, Chan SH, Jang TH, Chang JW, Ko YC, Yen TC, et al. miRNA-491-5p and GIT1 serve as modulators and biomarkers for oral squamous cell carcinoma invasion and metastasis. Cancer Res. 2014;74:751–64.
48. Sun R, Liu Z, Tong D, Yang Y, Guo B, Wang X, et al. miR-491-5p, mediated by Foxi1, functions as a tumor suppressor by targeting Wnt3a/β-catenin signaling in the development of gastric cancer. Cell Death Dis. 2017;8:e2714.
49. Xu Y, Hou R, Lu Q, Zhang Y, Chen L, Zheng Y, et al. MiR-491-5p negatively regulates cell proliferation and motility by targeting PDGFRA in prostate cancer. Am J Cancer Res. 2017;7:2545.
50. Kessenbrock K, Plaks V, Werb Z. Matrix metalloproteinases: regulators of the tumor microenvironment. Cell. 2010;141:52–67.
51. Kader AK, Shao L, Dinney CP, Schabath MB, Wang Y, Liu J, et al. Matrix metalloproteinase polymorphisms and bladder cancer risk. Cancer Res. 2006;66:11644–8.
52. Kader AK, Liu J, Shao L, Dinney CP, Lin J, Wang Y, et al. Matrix metalloproteinase polymorphisms are associated with bladder cancer invasiveness. Clin Cancer Res. 2007;13:2614–20.
53. Pirooz HJ, Jafari N, Rastegari M, Fathi-Roudsari M, Tasharrofi N, Shokri G, et al. Functional SNP in microRNA-491-5p binding site of MMP9 3′-UTR affects cancer susceptibility. J Cell Biochem. 2018;119:5126–34.
54. Ha M, Kim VN. Regulation of microRNA biogenesis. Nat Rev Mol Cell Biol. 2014;15:509–24.
55. Brockschmidt A, Trost D, Peterziel H, Zimmermann K, Ehrler M, Grassmann H, et al. KIAA1797/FOCAD encodes a novel focal adhesion protein with tumour suppressor function in gliomas. Brain. 2012;135:1027–41.
56. Weren RD, Venkatachalam R, Cazier JB, Farin HF, Kets CM, de Voer RM, et al. Germline deletions in the tumour suppressor gene FOCAD are associated with polyposis and colorectal cancer development. J Pathol. 2015;236:155–64.